An lncRNA-miRNA-mRNA ceRNA network for adipocyte differentiation from human adipose-derived stem cells

ZHEN GUO and YALI CAO

Department of Breast Surgery, The No. 3 Hospital of Nanchang, Nanchang, Jiangxi 330000, P.R. China

Received June 12, 2018; Accepted January 2, 2019

DOI: 10.3892/mmr.2019.10067

Abstract. Human adipose tissue-derived stromal stem cells (HASCs) represent a promising regenerative resource for breast reconstruction and augmentation. However, the mechanisms involved in inducing its adipogenic differentiation remain to be fully elucidated. The present study aimed to comprehensively investigate the expression changes in mRNAs, microRNAs (miRNAs) and long non-coding (lnc) RNAs during the adipogenic differentiation of HASCs, and screen crucial lncRNA-miRNA-mRNA interaction axes using microarray datasets GSE57593, GSE25715 and GSE61302 collected from the Gene Expression Omnibus database. Following pretreatment, differentially expressed genes (DEGs), miRNAs (DE-miRNAs) or lncRNAs (DE-lncRNAs) between undifferentiated and differentiated HASCs were identified using the Linear Models for Microarray data method. A protein-protein interaction (PPI) network was constructed for the DEGs based on protein databases, followed by module analysis. The 'lncRNA-miRNA-mRNA' competing endogenous RNA (ceRNA) network was constructed based on the interactions between miRNAs and mRNAs, lncRNAs and miRNAs predicted by the miRWalk and lnCeDB databases. The underlying functions of mRNAs were predicted using the clusterProfiler package. In the present study, 905 DEGs, 36 DE-miRNAs and 577 DE-lncRNAs were screened between undifferentiated HASCs and differentiated adipocyte cells. PPI network analysis demonstrated that LEP may be a hub gene, which was also enriched in significant module 5. LEP was predicted to be involved in the Janus kinase-signal transducer and activator of transcription signaling pathway, and the regulation of inflammatory response. The upregulation of LEP was regulated by downregulated hsa-miRNA (miR)-130b-5p and hsa-miR-23a-5p (or hsa-miR-302d-3p). These miRNAs also respectively interacted with RP11-552F3.9 (or RP11-15A1.7), ultimately forming the ceRNA axes. In conclusion, the present study revealed that the RP11-552F3.9 (RP11-15A1.7)-hsa-miR-130b-5p/hsa-miR-23a-5p (hsa-miR-302d-3p)-LEP interaction axes may be crucial for inducing the adipogenic differentiation of HASCs via involvement in inflammation.

Correspondence to: Dr Yali Cao, Department of Breast Surgery, The No. 3 Hospital of Nanchang, 2 Xiangshan South Road, Xihu, Nanchang, Jiangxi 330000, P.R. China
E-mail: yalicao2018@126.com

Key words: human adipose tissue-derived stromal stem cells, adipogenic differentiation, competing endogenous RNA, long non-coding RNA, microRNA

Introduction

Breast reconstruction and augmentation are frequently performed surgical procedures worldwide due to the high prevalence of breast cancer (1) and cosmetic demand. Autologous fat transfer to the subcutaneous tissue is the most commonly used technique in these plastic and reconstructive surgical procedures as it appears to be relatively inexpensive, readily obtainable, safe and complication-free compared with artificial implants (2). However, the long-term replacement outcomes may not be satisfactory, which may be, in part, attributed to low graft survival and poor vascularization (3). Therefore, it is necessary to further improve the autologous fat grafting technique to overcome the above limitations.

Human adipose-derived stem cells (HASCs) are a population of pluripotent cells, which have a high proliferation capacity, possess preferential potential to differentiate into adipocytes and can secrete angiogenic growth factors. Therefore, the addition of HASCs to lipoaspirate may prevent graft volume loss and enhance blood vessel generation in the grafts. This hypothesis has been confirmed in previous clinical trials (4-6). However, the use of autologous HASCs has not been Food and Drug Administration-approved; this may be due to the fact that the reconstructive mechanism of HASCs remains to be fully elucidated. Therefore, it is essential to investigate the molecular mechanisms that induce the transition of HASCs towards adipocytes and attempt to develop a more effective combination to improve the efficacy of HASC therapy for breast reconstruction and augmentation (7).

Currently, several genes have been identified to be associated with adipogenesis for HASCs. Cytokine interleukin-1α (IL-1α) is demonstrated to evidently inhibit the proliferation and adipogenic differentiation of HASCs through the activation of nuclear factor (NF)-κB and extracellular signal-regulated kinase 1/2 pathways; and subsequent upregulation of pro-inflammatory cytokines, including interleukin (IL)-8, IL-6, C-C motif chemokine

ligand 2 and IL-1β, in adipose-derived stem cells (8). A study by Strong *et al* (9) analyzed the overall cytokine profile of HASCs undergoing adipogenic differentiation and also found a decrease in the expression of IL-1, but reported increases in IL-12, IL-17 and intercellular adhesion molecule-1. By transcriptome profile analysis, Satish *et al* (10) identified several novel genes and signaling pathways involved in regulating adipogenesis, including periostin, protein phosphatase 1 regulatory inhibitor subunit 1A and fibroblast growth factor 11. MicroRNAs (miRNAs) are a class of small RNAs that are important for the regulation of cellular processes by downregulating gene expression via binding to the 3'-untranslated region. There is also evidence to indicate the roles of miRNAs in adipogenic differentiation. The levels of miRNA (miR)-27a and miR-27b have been found to be downregulated following the adipogenic induction of HASCs. The overexpression of miR-27a or miR-27b inhibits adipocyte differentiation by downregulating the expression of prohibitin; and the target association between miR-27a/b and prohibitin was confirmed using a luciferase reporter assay (11). miR-17-5p and miR-106a were shown to promote the adipogenic lineage commitment of HASCs by directly targeting bone morphogenetic protein 2 and subsequently increasing adipogenic CCAAT enhancer binding protein α (C/EBPα) and peroxisome proliferator activated receptor (PPAR)γ (12). In addition to miRNAs, long non-coding RNAs (lncRNAs) have emerged as important factors contributing to adipocyte differentiation in HASCs. Nuermaimaiti *et al* (13) demonstrated that the knockdown of HOXA11-AS1 inhibited adipocyte differentiation, leading to the suppression of adipogenic-related gene transcription in addition to decreased lipid accumulation in HASCs. The knockdown of MIR31HG also inhibited adipocyte differentiation, whereas the overexpression of MIR31HG promoted adipogenesis *in vitro* and *in vivo* (14). However, the adipogenic differentiation-related genes, miRNAs and lncRNAs of HASCs have received limited investigation.

Several scholars have put forward the competing endogenous RNAs (ceRNAs) hypothesis as an lncRNA-miRNA-mRNA link: LncRNAs may serve as molecular sponges for miRNAs and functionally liberate mRNA-targeted regulated by the aforementioned active miRNAs. Certain adipocyte differentiation-related lncRNA-miRNA-mRNA interaction axes have previously been obtained in bone marrow mesenchymal stem cells (BMSCs) (15,16), but not in HASCs.

The aim of the present study was to screen crucial miRNAs, lncRNAs and mRNAs associated with the adipocyte differentiation of HASCs by constructing the miRNA-lncRNA-mRNA ceRNA regulatory network using microarray data collected from a public database. The results of the present study may improve current understanding of the molecular mechanisms that induce the transition of HASCs towards adipocytes and provide targets for inducing adipogenic differentiation.

Materials and methods

Gene Expression Omnibus (GEO) dataset. The lncRNA, miRNA and mRNA expression profiles of HASCs prior to and following adipocyte differentiation were retrieved from the public GEO database (http://www.ncbi.nlm.nih.gov/geo/) under accession nos. GSE57593, GSE25715 and GSE61302 (10), respectively. The GSE57593 microarray dataset (platform: GPL18109, Agilent-038314 CBC Homo sapiens lncRNA + mRNA microarray V2.0) included samples from four undifferentiated HASCs and six differentiated adipocyte cells, which were induced following adipogenic medium culture for 3 and 6 days, with three replicates of each. The GSE25715 non-coding RNA sequencing dataset (platform: GPL9442, AB SOLiD System 3.0, Homo sapiens), included samples from four undifferentiated HASCs [two with adapter set A (from the 5' to the 3' end) and two with adapter set B (from the 3' to the 5' end)] and eight adipocyte differentiated cells that were induced using adipogenic medium for 3 and 8 days, with two replicates of each and using adapter sets A and B. The GSE61302 microarray dataset (platform: GPL570, Affymetrix Human Genome U133 Plus 2.0 Array) included samples from five undifferentiated HASCs and 10 differentiated adipocyte cells which were induced with adipogenic medium for 7 days (four replicates) and 21 days (six replicates).

Data preprocessing and differential expression analysis. For the microarray data, the raw data were preprocessed using the Robust Multichip Average algorithm (17) as implemented in the Bioconductor R package (version 3.4.1; http://www.bioconductor.org/packages/release/bioc/html/affy.html), including background correction, quantile normalization and median summarization. For the sequencing data, low expression value data (=0, 70%) were filtered.

In consideration of the different differentiated time, the present study only focused on the differentially expressed genes (DEGs), lncRNAs (DELs) and miRNAs (DEMs) between the undifferentiated and differentiated cells. The DEGs, DELs and DEMs were identified using the Linear Models for Microarray data method (18) in the Bioconductor R package (version 3.4.1; http://www.bioconductor.org/packages/release/bioc/html/limma.html). The empirical Bayes t-test was used to calculate the p-value, which was subsequently adjusted by the Benjamini-Hochberg (BH) procedure (19). Genes were considered differentially expressed if they met the following conditions: P-value (adjusted) $P<0.05$ and $|\log FC(\text{fold change})| > 1$ (that is, FC>2). A hierarchical cluster heatmap was created using the R package pheatmap (version: 1.0.8; https://cran.r-project.org/web/packages/pheatmap) based on the Euclidean distance to observe the ability of the DEGs, DELs and DEMs to distinguish the differentiated from the undifferentiated samples.

Protein-protein interaction (PPI) network. To screen crucial genes, the DEGs were imported into PPI data that were collected from the Search Tool for the Retrieval of Interacting Genes (version 10.0; http://string db.org/) database (20). The PPIs with combined scores ≥0.4 (medium confidence) were selected to construct the PPI network, which was visualized using Cytoscape software (version 3.4; www.cytoscape.org/) (21). The network topological features, including the degree (number of interactions per node or protein), betweenness (number of shortest paths that pass through each node), and closeness centrality (average length of the shortest paths to access all other proteins in the network) were determined using the CytoNCA plugin in Cytoscape software (http://apps.cytoscape.org/apps/cytonca) (22) to rank the

Table I. Top 10 upregulated and downregulated differentially expressed lncRNAs, miRNAs and mRNAs.

lncRNAs			miRNAs			mRNAs		
lncRNA	logFC	Adjusted P-value	miRNA	logFC	P-value	mRNA	logFC	Adjusted P-value
ZBED3-AS1	4.74	2.74×10^{-7}	hsa-miR-29b-2*	2.89	3.08×10^{-5}	FGF11	2.14	3.54×10^{-7}
RP11-95P13.1	4.95	5.72×10^{-7}	hsa-miR-642a-3p	5.28	4.29×10^{-4}	DDIT4L	3.38	4.11×10^{-7}
AC104654.2	4.12	1.08×10^{-5}	hsa-miR-2114	2.80	1.31×10^{-3}	PKP2	1.74	4.11×10^{-7}
RP11-196G18.3	2.19	1.41×10^{-5}	hsa-miR-30a*	2.54	2.20×10^{-3}	GPR155	1.57	4.11×10^{-7}
RP11-439A17.9	2.19	1.41×10^{-5}	hsa-miR-34b*	4.57	3.85×10^{-3}	ZNF582-AS1	1.20	4.11×10^{-7}
RP5-998N21.4	2.19	1.41×10^{-5}	hsa-miR-668	2.29	4.38×10^{-3}	PGRMC1	1.10	4.11×10^{-7}
CTC-564N23.2	4.65	2.62×10^{-5}	hsa-miR-345	1.81	4.20×10^{-3}	ZNF436-AS1	2.26	5.34×10^{-7}
CHL1-AS1	3.53	5.17×10^{-5}	hsa-miR-675*	2.60	5.68×10^{-3}	FAM162A	1.14	5.34×10^{-7}
AC104653.1	2.94	5.17×10^{-5}	hsa-miR-34a	3.54	8.48×10^{-3}	BNIP3	1.23	1.44×10^{-6}
RP11-696N14.1	2.15	5.17×10^{-5}	hsa-miR-378c	3.10	9.65×10^{-3}	IGFBP5	1.74	1.85×10^{-6}
LINC01085	-4.82	1.20×10^{-7}	hsa-miR-485-3p	-3.30	9.05×10^{-4}	FOSB	-6.71	1.28×10^{-14}
APCDD1L-AS1	-3.14	2.45×10^{-6}	hsa-miR-3151	-2.15	1.80×10^{-3}	IER2	-1.72	2.51×10^{-9}
RP11-54A9.1	-3.45	5.73×10^{-6}	hsa-miR-130b*	-1.42	6.82×10^{-3}	KLF2	-2.02	3.82×10^{-9}
CTD-2354A18.1	-3.16	7.55×10^{-6}	hsa-miR-302d	-1.66	8.82×10^{-3}	ID1	-4.29	1.64×10^{-8}
CTD-2066L21.2	-5.09	1.11×10^{-5}	hsa-miR-487a	-2.39	7.82×10^{-3}	SKIL	-1.49	4.79×10^{-8}
RP11-114H23.1	-1.83	1.11×10^{-5}	hsa-miR-411*	-1.31	4.96×10^{-2}	PRIMA1	-2.89	9.17×10^{-8}
RP3-410C9.2	-5.035	1.30×10^{-5}	hsa-miR-154*	-2.12	1.72×10^{-2}	RRM2	-4.51	9.17×10^{-8}
APOBEC3B-AS1	-3.97	1.30×10^{-5}	hsa-let-7e	-1.35	2.81×10^{-3}	EGR3	-5.27	9.17×10^{-8}
RP11-30P6.6	-3.10	1.41×10^{-5}	hsa-miR-125b-1*	-1.54	2.84×10^{-2}	C16orf89	-2.88	1.73×10^{-7}
LINC00460	-3.07	2.39×10^{-5}	hsa-miR-23b	-1.03	4.18×10^{-2}	NFKBIZ	-1.84	2.89×10^{-7}

lncRNA, long non-coding RNA; miRNA, microRNA.

nodes in the PPI network and screen hub genes. Modules were identified to be significant with an Molecular Complex Detection (MCODE) score ≥4 and ≥6 nodes.

Furthermore, the MCODE (version:1.4.2, http://apps.cytoscape.org/apps/mcode) plugin of Cytoscape software was also used to identify functionally related and highly interconnected modules from the PPI network with a degree cut-off of 2, node score cut-off of 0.2, k-core of 2 and maximum depth of 100 (23).

ceRNA regulatory network construction. The DEM-related target genes were predicted using the miRWalk database (version 2.0; http://www.zmf.umm.uni-heidelberg.de/apps/zmf/mirwalk2) (24), which provides the largest collection of predicted and experimentally verified miR-target interactions with various miRNA databases, including miRWalk, miRanda, miRDB, miRMap, RNA22 and TargetScan. The miRNA-target gene interaction pairs were selected if they were predicted in at least five databases. The target genes were then overlapped with the DEGs to screen the DEM (upregulated)-DEG (downregulated) or DEM (downregulated)-DEG (upregulated) interaction pairs.

The miRWalk (version 2.0; http://www.zmf.umm.uni-heidelberg.de/apps/zmf/mirwalk2) (24) and lnCeDB (http://gyanxet-beta.com/lncedb/) (25) databases were used to screen the interactions between DELs and DEMs. The DEL (upregulated)-DEM (downregulated) and DEL (downregulated)-DEM (upregulated) interaction pairs were collected.

The DEL-DEM and DEM-DEG interactions were integrated to construct the lncRNA-miRNA-mRNA ceRNA network, which was visualized using Cytoscape software (version 3.4; www.cytoscape.org/) (21).

Function enrichment analysis. Gene Ontology (GO) and Kyoto Encyclopedia of Genes and Genomes (KEGG) pathway enrichment analyses were performed using the clusterProfiler tool (version 3.2.11; http://www.bioconductor.org/packages/release/bioc/html/clusterProfiler.html) to reveal the function of the DEGs in the PPI and the target genes of miRNAs. Adjusted P<0.05 using the BH method was set as the cut-off value (19).

Results

Differential expression analysis. Based on the given threshold (adjusted P<0.05 and |logFC| >1), a total of 925 DEGs were identified from 20,514 mRNAs between the undifferentiated HASCs and differentiated adipocyte cells, including 302 upregulated and 623 downregulated DEGs; 577 DELs were screened from 7,882 lncRNAs between the undifferentiated HASCs and differentiated adipocyte cells, including 323 upregulated and 254 downregulated DELs. A

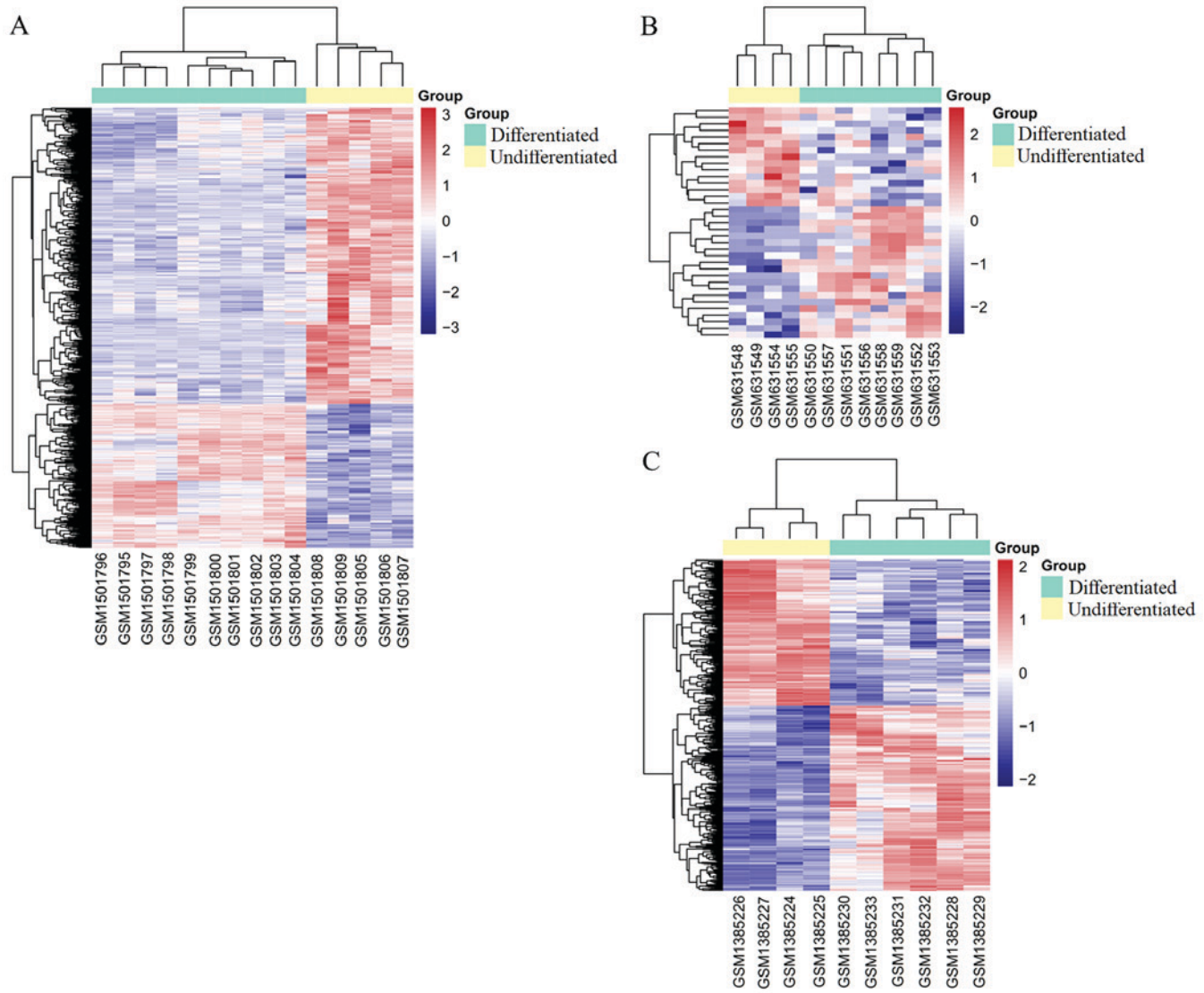

Figure 1. Hierarchical clustering and heatmap analysis of differentially expressed (A) genes, (B) microRNAs and (C) long non-coding RNAs. Red, high expression; blue, low expression.

total of 35 DEMs were screened from 499 miRNAs between the undifferentiated HASCs and differentiated adipocyte cells (including 20 upregulated and 15 downregulated), based on the threshold of P<0.05 and |logFC| >1. The top 20 DEGs, DEMs and DELs are shown in Table I. The heatmap indicated that these DEGs (Fig. 1A), DEMs (Fig. 1B) and DELs (Fig. 1C) distinguished the differentiated from the undifferentiated samples.

PPI network analysis of DEGs to screen hub genes. A PPI network was constructed using the screened DEGs, which included 360 nodes (162 upregulated and 198 downregulated) and 1,381 interaction pairs (Fig. 2). According to the rank of three topological features, JUN, cyclin B1 (CCNB1), C-X-C motif chemokine ligand 10 (CXCL10), enolase 2 (ENO2), enoyl-CoA hydratase and 3-hydroxyacyl CoA dehydrogenase (EHHADH), protein tyrosine phosphatase, receptor type C (PTPRC), Rac family small GTPase 2 (RAC2), leptin (LEP) and kinase insert domain receptor (KDR) were considered as hub genes in the PPI network (Table II). Six significant functionally related and highly interconnected modules were extracted from the whole PPI network (Fig. 3; Table III). Hub gene CCNB1 was enriched in module 1, which was associated with cell cycle (Fig. 3A). Hub gene CXCL10 was enriched in module 2 (Fig. 3B), which was associated with several inflammation pathways, including the chemokine signaling pathway, cytokine-cytokine receptor interaction, IL-17 signaling pathway, and tumor necrosis factor (TNF) signaling pathway. Hub gene ENO2 and PTPRC were respectively enriched into module 3 (Fig. 3C) and 4 (Fig. 3D). Hub gene JUN in module 4 was enriched in the NOD-like receptor signaling pathway or infection. Hub gene LEP in module 5 (Fig. 3E) was important in the Janus kinase (JAK)-signal transducer and activator of transcription (STAT) signaling pathway. Hub gene EHHADH in module 6 (Fig. 3F) was amino acid- or glucose metabolism-related (Table IV; Fig. 4A). As hub gene PTPRC and ENO2 were respectively enriched into module 4 and 3, but they were not included in the pathway-related genes, GO enrichment analysis was also performed. As a result, PTPRC was predicted to be involved

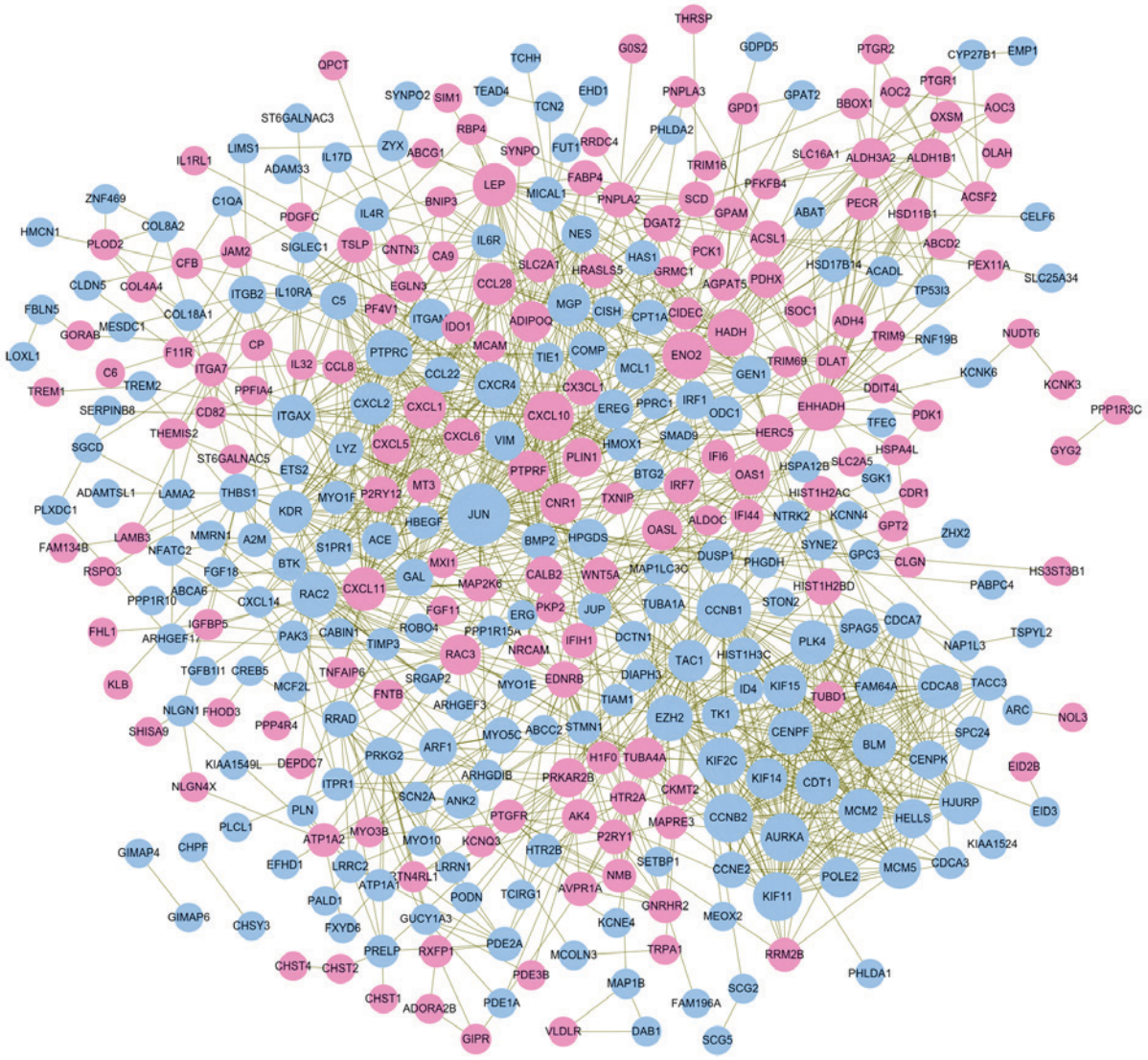

Figure 2. Protein-protein interaction network. Pink nodes, upregulated genes; light blue nodes, downregulated genes; brown line/edges, interaction between genes. A larger size of a node (protein) indicates it has a higher degree (number of interactions).

in positive regulation of cytosolic calcium ion concentration (Table V; Fig. 4B). The function of ENO2 was not predicted.

DEM-DEG regulatory association analysis. A total of 7,381 target genes were predicted for the 21 upregulated DEMs, and 5,841 were predicted for the 15 downregulated DEMs. Following overlapping with the DEGs, 654 interactions were obtained for the 21 upregulated DEMs and 247 downregulated DEGs, and 197 interactions were obtained for the 14 downregulated DEMs and 96 upregulated DEGs.

The target genes of five upregulated DEMs (hsa-miR-103a-2-5p, hsa-miR-582-5p, hsa-miR-642a-5p, hsa-miR-1292-5p and hsa-miR-30c-5p and) were enriched into 29 KEGG pathways, whereas 36 KEGG pathways were enriched for six downregulated DEMs (hsa-miR-302d-3p, hsa-miR-154-3p, hsa-miR-485-3p, hsa-miR-25-5p, hsa-miR-487a and hsa-miR-411-3p) (Fig. 5A). Among them, hsa-miR-302d-3p regulated hub gene LEP to be involved in neuroactive ligand-receptor interaction; whereas hsa-miR-487a targeted hub gene EHHADH for involvement in amino acid (β-alanine, lysine, valine, leucine and isoleucine) metabolism; hub gene CXCL10 regulated by hsa-miR-411-3p was involved in the IL-17 signaling pathway, Toll-like receptor signaling pathway, and TNF signaling pathway (Table VI).

Furthermore, GO biological process term enrichment analysis was also performed to predict the functions of DEMs (Fig. 5B). As a result, GO terms were enriched for nine upregulated DEMs (hsa-miR-103-5p, hsa-let-7e-5p, hsa-miR-212-3p, hsa-miR-345-5p, hsa-miR-378a-5p, hsa-miR-642a-3p, hsa-miR-582-3p, hsa-miR-664a-3p and hsa-miR-668-3p) and five downregulated DEMs (hsa-miR-302d-3p, hsa-miR-485-3p, hsa-miR-130b-5p, hsa-miR-23a-5p and hsa-miR-23b-5p). hsa-miR-378a-5p may regulate hub gene RAC2 to be involved in cell-substrate adhesion. hsa-miR-130b-5p, hsa-miR-23a-5p and hsa-miR-302d-3p may regulate hub gene LEP to be involved in regulation of inflammatory response and IL-8 secretion (Table VII).

ceRNA network. Using the miRWalk and InCeDB databases, 14 upregulated DEMs were predicted to regulate

Table II. Topological features of DEGs in the protein-protein interaction network.

DEG	Degree	DEG	Betweenness	DEG	Closeness	Overlapped	Expression
JUN	52	JUN	31682.11	JUN	0.12	JUN	Down
CCNB1	40	EHHADH	14484.48	PTPRC	0.12	CCNB1	Down
CXCL10	33	RAC2	9452.98	ENO2	0.12	CXCL10	Up
CCNB2	32	CCNB1	9055.00	CCNB1	0.12	ENO2	Up
AURKA	31	TAC1	8899.64	RAC2	0.12	EHHADH	Up
KIF11	31	ENO2	8383.99	KDR	0.12	PTPRC	Down
ENO2	30	KDR	7498.68	VIM	0.12	RAC2	Down
KIF2C	30	PTPRC	6640.64	EHHADH	0.12	LEP	UP
EHHADH	29	PRKAR2B	6288.09	HPGDS	0.12	KDR	Down
PTPRC	28	THBS1	5735.04	MCL1	0.12	ITGAM	Down
HADH	28	VIM	4843.88	TAC1	0.12	ITGAX	Down
RAC2	27	LEP	4442.09	CXCL10	0.11	CXCR4	Down
CXCR4	27	CXCL10	4424.07	MGP	0.11	HADH	Up
EZH2	27	HADH	4155.38	CXCR4	0.11	MGP	Down
MCM2	25	MGP	3982.14	LEP	0.11	TAC1	Down
PLK4	24	HPGDS	3752.53	BMP2	0.11		
CENPF	24	CNR1	3700.56	PTPRF	0.11		
CDCA8	24	PRKG2	3608.14	ADIPOQ	0.11		
LEP	23	CALB2	3569.40	WNT5A	0.11		
ITGAX	23	WNT5A	3556.75	ACE	0.11		
CXCL11	23	ITGAX	3251.43	ITGAM	0.11		
BLM	23	AK4	3154.06	THBS1	0.11		
KIF15	23	TUBA4A	2982.07	NES	0.11		
CDT1	23	HMOX1	2856.41	CPT1A	0.11		
KDR	22	PTPRF	2836.38	PLIN1	0.11		
MGP	22	ADIPOQ	2766.04	CX3CL1	0.11		
CCL28	22	ITGAM	2744.81	BTK	0.11		
HJURP	22	CXCR4	2674.93	MAP2K6	0.11		
TAC1	21	ITGA7	2632.36	CXCL2	0.11		
ITGAM	21	BMP2	2624.89	CXCL1	0.11		
CXCL2	21	PLIN1	2616.07	CALB2	0.11		
CXCL1	21	ACE	2575.42	ITGAX	0.11		
TUBA4A	20	ITGB2	2559.34	HADH	0.11		
MCM5	20	ALDH3A2	2510.02	IRF1	0.11		
MCL1	19	RRAD	2504.60	CCL28	0.11		

DEG, differentially expressed gene.

60 downregulated DELs and nine downregulated DEMs were predicted to regulate 15 upregulated DELs. An lncRNA-miRNA-mRNA ceRNA network was subsequently established (Fig. 6A and B), in which 366 nodes (23 DEMs: 14 upregulated and nine downregulated; 268 DEGs: 67 upregulated and 201 downregulated; 75 DELs: 15 upregulated and 60 downregulated) and 560 interactions (450 DEL-DEM and 110 DEM-DEG) were present. In this ceRNA, upregulated RP11-552F3.9 (or RP11-15A1.7) may function as a ceRNA to respectively suppress the inhibitory effects of hsa-miR-23a-5p and hsa-miR-302d-3p (or hsa-miR-130b-5p) on LEP, resulting in its upregulated expression; whereas the downregulation of GDNF-AS1 may be insufficient to prevent the inhibitory effects of hsa-miR-378a-5p on hub gene RAC2, leading to its downregulated expression (Fig. 6A and B).

Discussion

The present study aimed to identify crucial mRNAs, miRNAs and lncRNAs for the adipocyte differentiation of HASCs based on a series of bioinformatics analyses, including PPI network construction, module analysis, miRNA-mRNA regulatory pair prediction, ceRNA network generation and function enrichment. In these analyses, the LEP gene was enriched and was regulated by RP11-552F3.9 (or RP11-15A1.7)-hsa-miR-23a-5p/hsa-miR-302d-3p

Table III. Module analysis results.

Cluster	Score[a]	Nodes (n)	Edges (n)	Node IDs
1	17.89	19	161	HELLS, EZH2, HJURP, CDT1, CENPF, MCM2, POLE2, FAM64A, SPAG5, KIF2C, BLM, PLK4, CDCA8, KIF14, AURKA, KIF11, KIF15, CCNB1, CCNB2
2	13.00	13	78	CXCL10, GAL, CXCL5, CXCL11, C5, P2RY12, CCL28, CNR1, S1PR1, CXCL2, CXCL1, CXCR4, CXCL6
3	9.78	10	44	GEN1, COMP, HADH, PTPRF, HRASLS5, ENO2, MCL1, MGP, EREG, NES
4	7.00	21	70	OAS1, JUN, GNRHR2, AVPR1A, P2RY1, ITGAM, CCL22, HERC5, EDNRB, OASL, PTGFR, IFIH1, PTPRC, IRF7, IFI44, HTR2A, ITGAX, TAC1, IFI6, NMB, HTR2B
5	4.67	10	21	ACSL1, SCD, DGAT2, PNPLA2, LEP, CIDEC, IL4R, IL10RA, TSLP, FABP4
6	4.36	12	24	TUBA1A, PRKAR2B, ABAT, EHHADH, ALDH3A2, TUBD1, ALDH1B1, MAPRE3, PECR, PDHX, TUBA4A, HSD11B1
7	3.33	4	5	PDE2A, PRELP, RRAD, LRRC2
8	3.13	17	25	MMRN1, ANK2, ATP1A2, NRCAM, VIM, KDR, ATP1A1, PLOD2, TIMP3, COL8A2, COL4A4, CALB2, PLN, KCNQ3, A2M, COL18A1, SCN2A
9	3.00	3	3	HIST1H3C, HIST1H2AC, HIST1H2BD
10	3.00	3	3	HSD17B14, ADH4, TP53I3
11	3.00	3	3	TRIM69, RNF19B, TRIM9
12	3.00	3	3	GPAT2, AGPAT5, GPD1
13	3.00	3	3	VLDLR, DAB1, MAP1B
14	3.00	3	3	LAMB3, ITGA7, LAMA2

[a]Score = density x number of nodes.

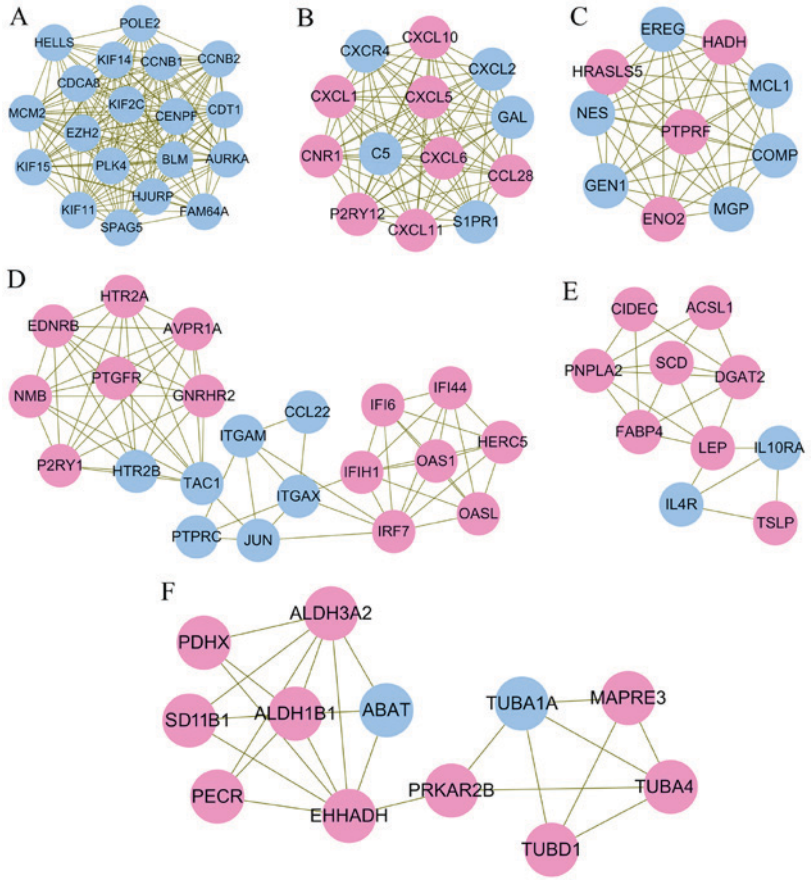

Figure 3. Significant modules extracted from the protein-protein interaction network. (A) Module 1; (B) module 2; (C) module 3; (D) module 4; (E) module 5; (F) module 6.

Table IV. Kyoto Encyclopedia of Genes and Genomes pathway enrichment for genes in modules.

Cluster	ID	Description	Adjusted P-value	Genes
1	hsa04914	Progesterone-mediated oocyte maturation	$1.16x10^{-3}$	AURKA/CCNB1/CCNB2
1	hsa04110	Cell cycle	$1.16x10^{-3}$	MCM2/CCNB1/CCNB2
1	hsa04114	Oocyte meiosis	$1.16x10^{-3}$	AURKA/CCNB1/CCNB2
1	hsa04068	FoxO signaling pathway	$1.16x10^{-3}$	PLK4/CCNB1/CCNB2
1	hsa03030	DNA replication	$2.02x10^{-3}$	MCM2/POLE2
1	hsa04115	p53 signaling pathway	$5.99x10^{-3}$	CCNB1/CCNB2
1	hsa04218	Cellular senescence	$2.73x10^{-2}$	CCNB1/CCNB2
2	hsa04062	Chemokine signaling pathway	$1.96x10^{-9}$	CXCL10/CXCL5/CXCL11/CCL28/CXCL2/CXCL1/CXCR4/CXCL6
2	hsa04060	Cytokine-cytokine receptor interaction	$2.03x10^{-8}$	CXCL10/CXCL5/CXCL11/CCL28/CXCL2/CXCL1/CXCR4/CXCL6
2	hsa04657	IL-17 signaling pathway	$2.28x10^{-6}$	CXCL10/CXCL5/CXCL2/CXCL1/CXCL6
2	hsa04668	TNF signaling pathway	$1.60x10^{-4}$	CXCL10/CXCL5/CXCL2/CXCL1
2	hsa05133	Pertussis	$1.41x10^{-3}$	CXCL5/C5/CXCL6
2	hsa05323	Rheumatoid arthritis	$1.94x10^{-3}$	CXCL5/CXCL1/CXCL6
2	hsa04672	Intestinal immune network for IgA production	$1.28x10^{-2}$	CCL28/CXCR4
2	hsa05134	Legionellosis	$1.41x10^{-2}$	CXCL2/CXCL1
2	hsa05132	Salmonella infection	$0.02.99x10^{-2}$	CXCL2/CXCL1
2	hsa04620	Toll-like receptor signaling pathway	$3.88x10^{-2}$	CXCL10/CXCL11
4	hsa04080	Neuroactive ligand-receptor interaction	$7.99x10^{-4}$	AVPR1A/P2RY1/EDNRB/PTGFR/HTR2A/HTR2B
4	hsa04020	Calcium signaling pathway	$8.35x10^{-4}$	AVPR1A/EDNRB/PTGFR/HTR2A/HTR2B
4	hsa05164	Influenza A	$8.30x10^{-3}$	OAS1/JUN/IFIH1/IRF7
4	hsa05168	Herpes simplex infection	$8.30x10^{-3}$	OAS1/JUN/IFIH1/IRF7
4	hsa05162	Measles	$3.60x10^{-2}$	OAS1/IFIH1/IRF7
4	hsa05161	Hepatitis B	$3.68x10^{-2}$	JUN/IFIH1/IRF7
4	hsa04621	NOD-like receptor signaling pathway	$4.88x10^{-2}$	OAS1/JUN/IRF7
5	hsa04630	Jak-STAT signaling pathway	$6.39x10^{-4}$	LEP/IL4R/IL10RA/TSLP
5	hsa03320	PPAR signaling pathway	$8.88x10^{-4}$	ACSL1/SCD/FABP4
5	hsa04060	Cytokine-cytokine receptor interaction	$1.57x10^{-3}$	LEP/IL4R/IL10RA/TSLP
5	hsa01212	Fatty acid metabolism	$9.00x10^{-3}$	ACSL1/SCD
5	hsa04923	Regulation of lipolysis in adipocytes	$9.10x10^{-3}$	PNPLA2/FABP4
5	hsa00561	Glycerolipid metabolism	$9.65x10^{-3}$	DGAT2/PNPLA2
5	hsa04920	Adipocytokine signaling pathway	$0.01.06x10^{-2}$	ACSL1/LEP
5	hsa04152	AMPK signaling pathway	$2.76x10^{-2}$	SCD/LEP
5	hsa00061	Fatty acid biosynthesis	$4.36x10^{-2}$	ACSL1
6	hsa00410	β-alanine metabolism	$1.50x10^{-6}$	ABAT/EHHADH/ALDH3A2/ALDH1B1
6	hsa00280	Valine, leucine and isoleucine degradation	$4.60x10^{-6}$	ABAT/EHHADH/ALDH3A2/ALDH1B1
6	hsa00380	Tryptophan metabolism	$1.65x10^{-4}$	EHHADH/ALDH3A2/ALDH1B1
6	hsa00071	Fatty acid degradation	$1.66x10^{-4}$	EHHADH/ALDH3A2/ALDH1B1
6	hsa00310	Lysine degradation	$3.22x10^{-4}$	EHHADH/ALDH3A2/ALDH1B1
6	hsa00340	Histidine metabolism	$1.98x10^{-3}$	ALDH3A2/ALDH1B1
6	hsa00053	Ascorbate and aldarate metabolism	$2.21x10^{-3}$	ALDH3A2/ALDH1B1
6	hsa00650	Butanoate metabolism	$2.21x10^{-3}$	ABAT/EHHADH
6	hsa00640	Propanoate metabolism	$2.57x10^{-3}$	ABAT/EHHADH
6	hsa00620	Pyruvate metabolism	$3.44x10^{-3}$	ALDH3A2/ALDH1B1
6	hsa01212	Fatty acid metabolism	$4.70x10^{-3}$	EHHADH/PECR
6	hsa00330	Arginine and proline metabolism	$4.70x10^{-3}$	ALDH3A2/ALDH1B1

Table IV. Continued.

Cluster	ID	Description	Adjusted P-value	Genes
6	hsa05130	Pathogenic *Escherichia coli* infection	$5.24x10^{-3}$	TUBA1A/TUBA4A
6	hsa00561	Glycerolipid metabolism	$6.00x10^{-3}$	ALDH3A2/ALDH1B1
6	hsa00010	Glycolysis/Gluconeogenesis	$6.90x10^{-3}$	ALDH3A2/ALDH1B1
6	hsa04146	Peroxisome	$9.55x10^{-3}$	EHHADH/PECR
6	hsa04540	Gap junction	$1.01x10^{-2}$	TUBA1A/TUBA4A
6	hsa04210	Apoptosis	$2.27x10^{-2}$	TUBA1A/TUBA4A
6	hsa04145	Phagosome	$2.58x10^{-2}$	TUBA1A/TUBA4A
6	hsa04530	Tight junction	$3.03x10^{-2}$	TUBA1A/TUBA4A
6	hsa01040	Biosynthesis of unsaturated fatty acids	$4.23x10^{-2}$	PECR

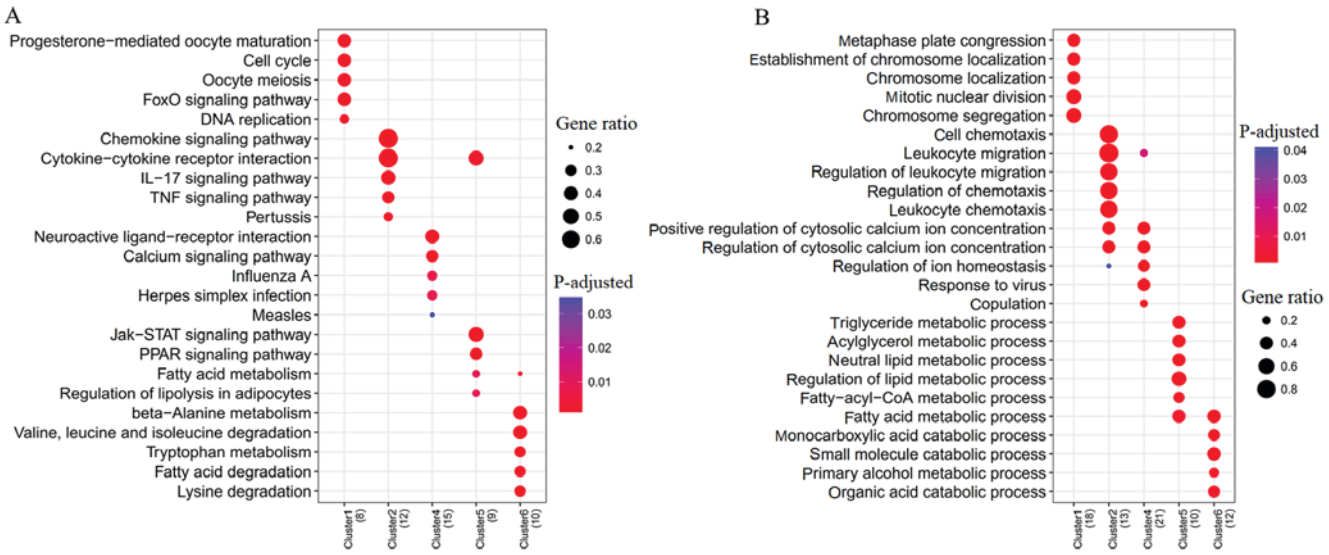

Figure 4. Pathway and GO term enrichment of gene clusters. (A) Kyoto Encyclopedia of Genes and Genomes pathway and (B) GO term enrichment analyses for genes of significant modules. The values within brackets are the number of genes enriched. GO, Gene Ontology.

(or hsa-miR-130b-5p), and involved in the inflammatory response, indicating that the LEP-related ceRNA axis may be important for the differentiation of adipose tissue-derived stem cells into adipocytes.

There is evidence demonstrating that LEP is important in adipocyte differentiation (26). Lee *et al* (27) observed that leptin treatment can promote lipid droplet formation and adipocyte differentiation, which was evaluated by the activity of glycerol-3-phosphate dehydrogenase activity, of HASCs. Additionally, the effect of leptin on adipocyte differentiation was found to be higher for HASCs than BMSCs (27). Another study indicated that, in BMSCs, leptin may accelerate osteogenic differentiation but inhibit adipocyte differentiation (28). Similarly, leptin was shown to have a suppressive effect on adipogenesis in dental pulp stem cells and periodontal ligament stem cells (29). These findings suggest that leptin may be a specific factor for regeneration of the subcutaneous fat layer using HASCs for tissue engineering. As expected, the LEP gene was also significantly upregulated in differentiated adipocyte samples compared with undifferentiated HASCs in the present study. It was predicted that the downstream of LEP may be involved in the JAK-STAT signaling pathway to mediate the inflammatory response via interaction with certain anti-inflammatory-related factors (IL4R, downregulated; Table IV; Fig. 3E). This prediction appears to have been indirectly verified by previous studies; it has been reported that leptin may have a promoting effect on the astroglial differentiation of stem cells through activation of the JAK-STAT pathway, with JAK-STAT inhibitors decreasing the expression of astrocyte marker leptin (30). STAT6 is reported to inhibit human IL-4 promoter activity in T cells and downregulate the gene expression of IL-4 (31). IL-4/IL4R can inhibit adipocyte differentiation by two mechanisms: Inhibiting adipogenesis via downregulating the expression of PPARγ and C/EBPα; and promoting lipolysis in mature adipocytes via enhancing the activity and translocation of hormone-sensitive lipase to decrease lipid deposits (32). However, the LEP-JAK-STAT-IL-4/IL4R signal pathways in the adipocyte differentiation of HASCs requires further experimental validation. In addition to the downstream pathways, the present

Table V. GO enrichment for genes in modules.

Cluster	ID	Description	Adjusted P-value	Genes
1	GO:0051310	Metaphase plate congression	$4.09x10^{-11}$	CDT1/CENPF/SPAG5/KIF2C/CDCA8/KIF14/CCNB1
1	GO:0051303	Establishment of chromosome localization	$1.45x10^{-10}$	CDT1/CENPF/SPAG5/KIF2C/CDCA8/KIF14/CCNB1
1	GO:0050000	Chromosome localization	$1.45x10^{-10}$	CDT1/CENPF/SPAG5/KIF2C/CDCA8/KIF14/CCNB1
1	GO:0140014	Mitotic nuclear division	$1.71x10^{-10}$	CDT1/CENPF/SPAG5/KIF2C/CDCA8/KIF14/AURKA/KIF11/CCNB1
1	GO:0000280	Nuclear division	$5.46x10^{-9}$	CDT1/CENPF/SPAG5/KIF2C/CDCA8/KIF14/AURKA/KIF11/CCNB1
2	GO:0060326	Cell chemotaxis	$9.21x10^{-14}$	CXCL10/CXCL5/CXCL11/C5/CCL28/S1PR1/CXCL2/CXCL1/CXCR4/CXCL6
2	GO:0050900	Leukocyte migration	$9.21x10^{-14}$	CXCL10/CXCL5/CXCL11/C5/P2RY12/CCL28/S1PR1/CXCL2/CXCL1/CXCR4/CXCL6
2	GO:0002685	Regulation of leukocyte migration	$9.21x10^{-14}$	CXCL10/CXCL5/CXCL11/C5/P2RY12/CCL28/CXCL2/CXCL1/CXCL6
2	GO:0050920	Regulation of chemotaxis	$1.35x10^{-13}$	CXCL10/CXCL5/CXCL11/C5/S1PR1/CXCL2/CXCL1/CXCR4/CXCL6
2	GO:0030595	Leukocyte chemotaxis	$2.66x10^{-13}$	CXCL10/CXCL5/CXCL11/C5/S1PR1/CXCL2/CXCL1/CXCR4/CXCL6
4	GO:0007204	Positive regulation of cytosolic calcium ion concentration	$6.33x10^{-7}$	AVPR1A/P2RY1/EDNRB/PTPRC/HTR2A/TAC1/NMB/HTR2B
4	GO:0009615	Response to virus	$6.33x10^{-7}$	OAS1/CCL22/HERC5/OASL/IFIH1/PTPRC/IRF7/IFI44
4	GO:0051480	Regulation of cytosolic calcium ion concentration	$6.33x10^{-7}$	AVPR1A/P2RY1/EDNRB/PTPRC/HTR2A/TAC1/NMB/HTR2B
4	GO:2000021	Regulation of ion homeostasis	$8.55x10^{-7}$	AVPR1A/EDNRB/PTPRC/HTR2A/TAC1/IFI6/HTR2B
4	GO:0007620	Copulation	$1.45x10^{-6}$	AVPR1A/P2RY1/EDNRB/TAC1
5	GO:0006641	Triglyceride metabolic process	$8.23x10^{-5}$	ACSL1/DGAT2/PNPLA2/FABP4
5	GO:0006639	Acylglycerol metabolic process	$8.23x10^{-5}$	ACSL1/DGAT2/PNPLA2/FABP4
5	GO:0006638	Neutral lipid metabolic process	$8.23x10^{-5}$	ACSL1/DGAT2/PNPLA2/FABP4
5	GO:0019216	Regulation of lipid metabolic process	$1.38x10^{-4}$	ACSL1/SCD/DGAT2/PNPLA2/LEP
5	GO:0035337	Fatty-acyl-CoA metabolic process	$1.60x10^{-4}$	ACSL1/SCD/DGAT2
6	GO:0072329	Monocarboxylic acid catabolic process	$2.81x10^{-4}$	ABAT/EHHADH/ALDH3A2/PECR
6	GO:0006631	Fatty acid metabolic process	$2.81x10^{-4}$	PRKAR2B/EHHADH/ALDH3A2/PECR/PDHX
6	GO:0044282	Small molecule catabolic process	$2.81x10^{-4}$	ABAT/EHHADH/ALDH3A2/ALDH1B1/PECR
6	GO:0034308	Primary alcohol metabolic process	$5.03x10^{-4}$	ALDH3A2/ALDH1B1/PECR
6	GO:0016054	Organic acid catabolic process	$8.48x10^{-4}$	ABAT/EHHADH/ALDH3A2/PECR

Only the top five terms are listed. GO, Gene Ontology.

study also analyzed the upstream non-coding RNAs of LEP, including miRNAs and lncRNAs, which were previously considered to be crucial for the adipogenic differentiation of HASCs (13,14,33-36). The results identified the RP11-552F3.9 (or RP11-15A1.7)-hsa-miR-23a-5p/hsa-miR-302d-3p (or hsa-miR-130b-5p)-LEP ceRNA axes. miR-130 has been shown to affect adipocyte differentiation from preadipocytes, with overexpressing miR-130 impairing adipogenesis and reducing miR-130-enhanced adipogenesis, and its potential target may be adipogenesis-related gene PPARγ (37). In addition, the inhibition of miR-23a has been reported to increase the adipogenic differentiation of BMSCs (38). In line with these findings, the present study found that hsa-miR-130b-5p and has-miR-23a-5p were downregulated in adipocyte differentiated HASCs. There have been no reports on the roles of miR-302d-3p and the above lncRNAs (RP11-552F3.9 and

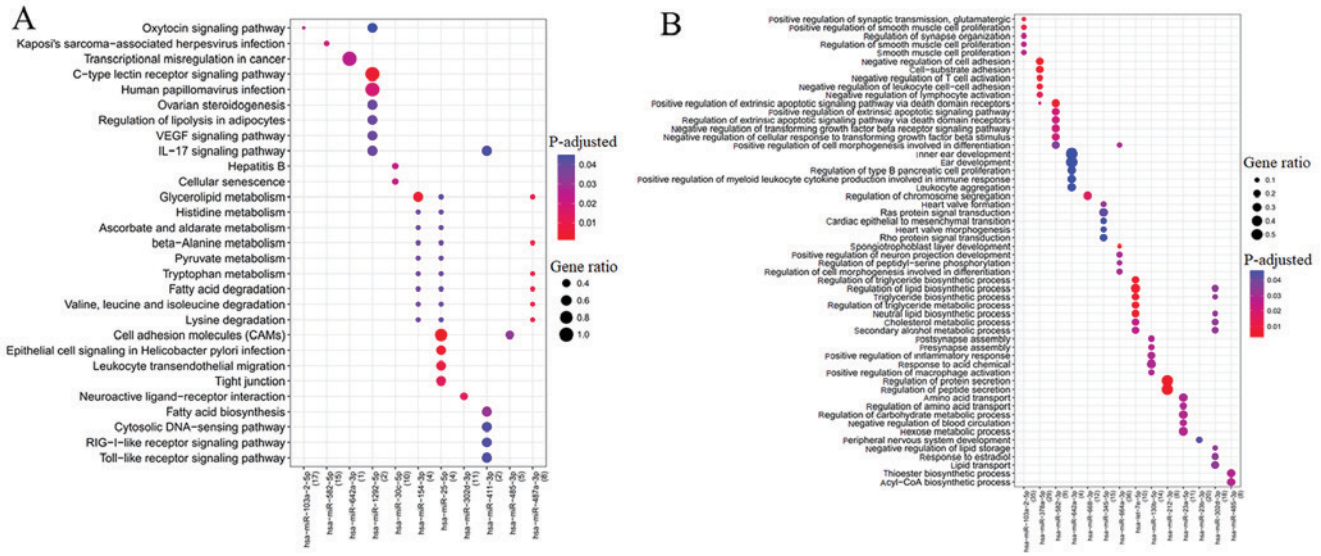

Figure 5. Pathway and GO term enrichment of microRNAs. (A) Kyoto Encyclopedia of Genes and Genomes pathway and (B) GO term enrichment analyses for target genes of differentially expressed microRNAs. The values within brackets are the number of genes enriched. miR, microRNA; GO, Gene Ontology.

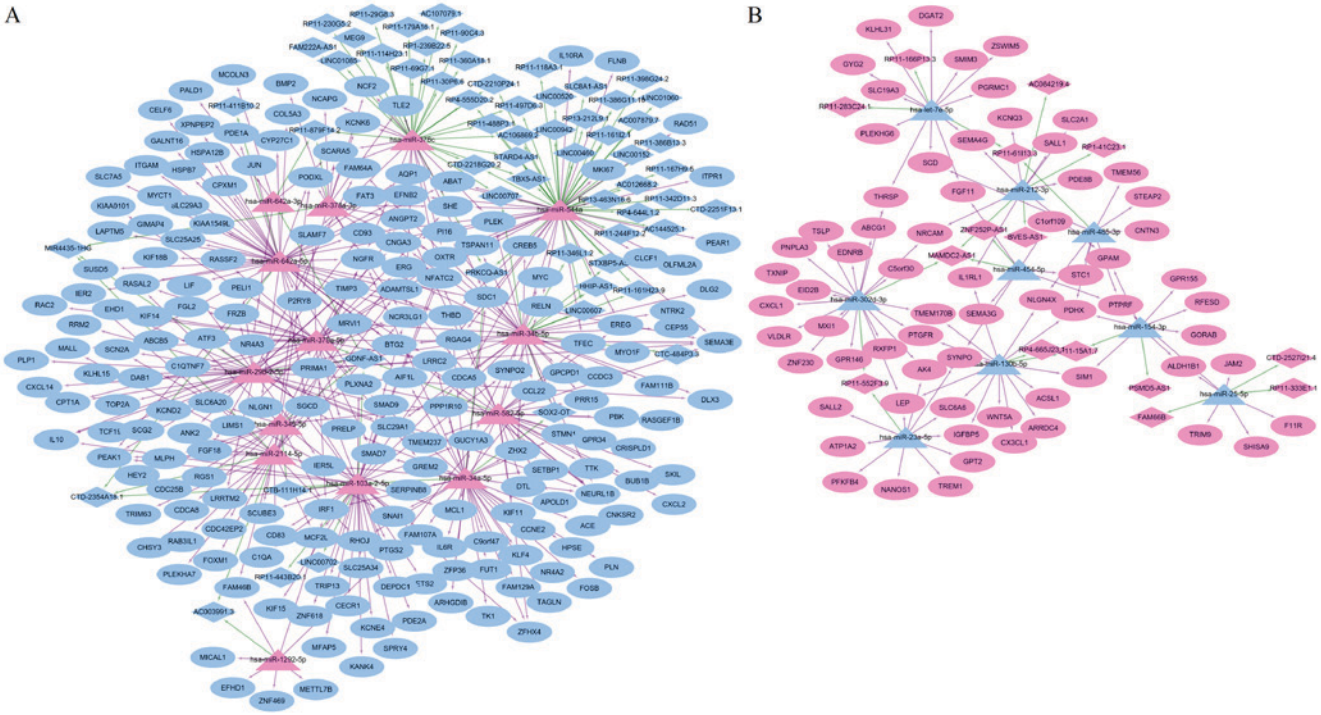

Figure 6. ceRNA interaction network of lncRNA-miRNA-mRNAs in human adipose-derived stem cells. (A) Downregulated lncRNA-related ceRNA network; (B) upregulated lncRNA-related ceRNA network. Diamond nodes represent lncRNAs; triangle nodes represent miRNAs; oval nodes represent mRNAs. Edges represent the possible associations between lncRNAs, miRNAs and mRNAs. Pink, upregulated; light blue, downregulated. ceRNA, competing endogenous RNAs; lncRNA, long non-coding RNA; miRNA, microRNA.

RP11-15A1.7) for adipocyte differentiation, indicating they may be novel targets identified by the present study.

RAC2 was identified as another hub gene that may be involved in the adipocyte differentiation of HASCs by miRNA-mRNA regulatory pair prediction and ceRNA network analysis. RAC2 was related to cell-substrate adhesion. It is well accepted that cell-substrate adhesion can control the fate of stem cells (39). A previous study showed that HASCs differentiated into adipocytes when the substrate stiffness decreased (40). Focal adhesion kinase (FAK) is a central protein involved in cell-substrate adhesion by Cas-Rac-lamellipodin signaling (41). The stimulation of Rac and increase in the activity of FAK enhanced cell tension by maintaining cell shape and matrix adhesion (42), whereas reduced cell stiffness and reduced adhesion strength have been observed in FAK-deficient cells (43). The inhibition of FAK has also been reported to lead to the elevation of adipogenic marker gene LEP and lipid accumulation in HASCs (43). These findings

Table VI. Kyoto Encyclopedia of Genes and Genomes pathway enrichment for target genes of microRNAs.

Expression	Cluster	ID	Description	Adjusted P-value	Genes
Up	hsa-miR-103a-2-5p	hsa04921	Oxytocin signaling pathway	2.67×10^{-2}	NFATC2/OXTR/ GUCY1A3/PTGS2
	hsa-miR-582-5p	hsa05167	Kaposi's sarcoma-associated herpesvirus infection	2.16×10^{-2}	PTGS2/ANGPT2/ CXCL2/NFATC2
	hsa-miR-642a-3p	hsa05202	Transcriptional misregulation in cancer	2.51×10^{-2}	NR4A3
	hsa-miR-1292-5p	hsa04625	C-type lectin receptor signaling pathway	3.91×10^{-3}	PTGS2/IRF1
	hsa-miR-1292-5p	hsa05165	Human papillomavirus infection	1.85×10^{-2}	PTGS2/IRF1
	hsa-miR-1292-5p	hsa04923	Regulation of lipolysis in adipocytes	3.92×10^{-2}	PTGS2
	hsa-miR-1292-5p	hsa04370	VEGF signaling pathway	3.92×10^{-2}	PTGS2
	hsa-miR-1292-5p	hsa04917	Prolactin signaling pathway	3.92×10^{-2}	IRF1
	hsa-miR-1292-5p	hsa05140	Leishmaniasis	3.92×10^{-2}	PTGS2
	hsa-miR-1292-5p	hsa05133	Pertussis	3.92×10^{-2}	IRF1
	hsa-miR-1292-5p	hsa04657	IL-17 signaling pathway	3.92×10^{-2}	PTGS2
	hsa-miR-1292-5p	hsa04064	NF-κB signaling pathway	3.92×10^{-2}	PTGS2
	hsa-miR-1292-5p	hsa04668	TNF signaling pathway	4.04×10^{-2}	PTGS2
	hsa-miR-1292-5p	hsa05160	Hepatitis C	4.38×10^{-2}	IRF1
	hsa-miR-30c-5p	hsa05161	Hepatitis B	2.34×10^{-2}	NFATC2/CCNA1/CCNE2
	hsa-miR-30c-5p	hsa04218	Cellular senescence	2.34×10^{-2}	NFATC2/CCNA1/CCNE2
Down	hsa-miR-154-3p	hsa00561	Glycerolipid metabolism	5.15×10^{-3}	GPAM/ALDH1B1
	hsa-miR-154-3p	hsa00340	Histidine metabolism	3.86×10^{-2}	ALDH1B1
	hsa-miR-154-3p	hsa00053	Ascorbate and aldarate metabolism	3.86×10^{-2}	ALDH1B1
	hsa-miR-154-3p	hsa00410	β-alanine metabolism	3.86×10^{-2}	ALDH1B1
	hsa-miR-154-3p	hsa00620	Pyruvate metabolism	3.86×10^{-2}	ALDH1B1
	hsa-miR-25-5p	hsa04514	Cell adhesion molecules (CAMs)	5.22×10^{-4}	PTPRF/F11R/JAM2
	hsa-miR-25-5p	hsa05120	Epithelial cell signaling in Helicobacter pylori infection	4.44×10^{-3}	F11R/JAM2
	hsa-miR-25-5p	hsa04670	Leukocyte transendothelial migration	8.00×10^{-3}	F11R/JAM2
	hsa-miR-25-5p	hsa04530	Tight junction	1.37×10^{-2}	F11R/JAM2
	hsa-miR-25-5p	hsa00340	Histidine metabolism	4.01×10^{-2}	ALDH1B1
	hsa-miR-302d-3p	hsa04080	Neuroactive ligand-receptor interaction	1.35×10^{-2}	EDNRB/LEP/RXFP1/ PTGFR
	hsa-miR-485-3p	hsa04514	Cell adhesion molecules (CAMs)	3.30×10^{-2}	PTPRF/NLGN4X
	hsa-miR-487a-3p	hsa00410	β-alanine metabolism	1.07×10^{-2}	ALDH1B1/EHHADH
	hsa-miR-487a-3p	hsa00380	Tryptophan metabolism	1.07×10^{-2}	ALDH1B1/EHHADH
	hsa-miR-487a-3p	hsa00071	Fatty acid degradation	1.07×10^{-2}	ALDH1B1/EHHADH
	hsa-miR-487a-3p	hsa00280	Valine, leucine and isoleucine degradation	1.07×10^{-2}	ALDH1B1/EHHADH
	hsa-miR-487a-3p	hsa00310	Lysine degradation	1.15×10^{-2}	ALDH1B1/EHHADH
	hsa-miR-487a-3p	hsa00561	Glycerolipid metabolism	1.15×10^{-2}	GPAM/ALDH1B1
	hsa-miR-411-3p	hsa00061	Fatty acid biosynthesis	3.16×10^{-2}	OLAH
	hsa-miR-411-3p	hsa04623	Cytosolic DNA-sensing pathway	4.34×10^{-2}	CXCL10
	hsa-miR-411-3p	hsa04622	RIG-I-like receptor signaling pathway	4.34×10^{-2}	CXCL10
	hsa-miR-411-3p	hsa04657	IL-17 signaling pathway	4.34×10^{-2}	CXCL10
	hsa-miR-411-3p	hsa04620	Toll-like receptor signaling pathway	4.34×10^{-2}	CXCL10
	hsa-miR-411-3p	hsa04668	TNF signaling pathway	4.34×10^{-2}	CXCL10

miR, microRNA.

implicate the underlying anti-adipogenic activity of FAK and RAC. In line with these findings, the present study found that RAC2 was downregulated in adipocyte differentiated HASCs. Furthermore, it was predicted that RAC2 may be regulated by GDNF-AS1-hsa-miR-378a-5p. Previous evidence has shown that miR-378 is an adipogenesis-related miRNA in human

Table VII. GO term enrichment for target genes of microRNAs.

Expression	Cluster	ID	Description	Adjusted P-value	Genes
Up	hsa-miR-103a-2-5p	GO:0051968	Positive regulation of synaptic transmission, glutamatergic	$1.18x10^{-2}$	OXTR/NLGN1/PTGS2
	hsa-miR-103a-2-5p	GO:0048661	Positive regulation of smooth muscle cell proliferation	$1.18x10^{-2}$	IL10/NR4A3/IL6R/PTGS2
	hsa-miR-103a-2-5p	GO:0050807	Regulation of synapse organization	$2.79x10^{-2}$	OXTR/IL10/NLGN1/LRRTM2
	hsa-miR-103a-2-5p	GO:0048660	Regulation of smooth muscle cell proliferation	$2.79x10^{-2}$	IL10/NR4A3/IL6R/PTGS2
	hsa-miR-103a-2-5p	GO:0048659	Smooth muscle cell proliferation	$2.79x10^{-2}$	IL10/NR4A3/IL6R/PTGS2
	hsa-miR-378a-5p	GO:0007162	Negative regulation of cell adhesion	$3.27x10^{-3}$	IRF1/PELI1/ANGPT2/IL10/SMAD7/SEMA3E
	hsa-miR-378a-5p	GO:0031589	Cell-substrate adhesion	$6.55x10^{-3}$	LIMS1/RAC2/KIF14/ANGPT2/SEMA3E/PEAK1
	hsa-miR-378a-5p	GO:0050868	Negative regulation of T cell activation	$8.67x10^{-3}$	IRF1/PELI1/IL10/SMAD7
	hsa-miR-378a-5p	GO:1903038	Negative regulation of leukocyte cell-cell adhesion	$9.77x10^{-3}$	IRF1/PELI1/IL10/SMAD7
	hsa-miR-378a-5p	GO:0051250	Negative regulation of lymphocyte activation	$1.53x10^{-2}$	IRF1/PELI1/IL10/SMAD7
	hsa-miR-582-3p	GO:1902043	Positive regulation of extrinsic apoptotic signaling pathway via death domain receptors	$6.49x10^{-3}$	SKIL/TIMP3
	hsa-miR-582-3p	GO:2001238	Positive regulation of extrinsic apoptotic signaling pathway	$2.23x10^{-2}$	SKIL/TIMP3
	hsa-miR-582-3p	GO:1902041	Regulation of extrinsic apoptotic signaling pathway via death domain receptors	$2.23x10^{-2}$	SKIL/TIMP3
	hsa-miR-582-3p	GO:0030512	Negative regulation of transforming growth factor β receptor signaling pathway	$2.23x10^{-2}$	SKIL/HTRA4
	hsa-miR-582-3p	GO:1903845	Negative regulation of cellular response to transforming growth factor β stimulus	$2.23x10^{-2}$	SKIL/HTRA4
	hsa-miR-642a-3p	GO:0048839	Inner ear development	$4.66x10^{-2}$	NR4A3/MCOLN3
	hsa-miR-642a-3p	GO:0043583	Ear development	$4.66x10^{-2}$	NR4A3/MCOLN3
	hsa-miR-642a-3p	GO:0061469	Regulation of type B pancreatic cell proliferation	$4.66x10^{-2}$	NR4A3
	hsa-miR-642a-3p	GO:0061081	Positive regulation of myeloid leukocyte cytokine production involved in immune response	$4.66x10^{-2}$	NR4A3
	hsa-miR-642a-3p	GO:0070486	Leukocyte aggregation	$4.66x10^{-2}$	NR4A3
	hsa-miR-668-3p	GO:0051983	Regulation of chromosome segregation	$1.74x10^{-2}$	KIF2C/MKI67/GEN1
	hsa-miR-345-5p	GO:0003188	Heart valve formation	$3.30x10^{-2}$	HEY2/ERG
	hsa-miR-345-5p	GO:0007265	Ras protein signal transduction	$4.24x10^{-2}$	CDC42EP2/NGFR/RASAL2/P2RY8
	hsa-miR-345-5p	GO:0060317	Cardiac epithelial to mesenchymal transition	$4.65x10^{-2}$	HEY2/ERG

Table VII. Continued.

Expression	Cluster	ID	Description	Adjusted P-value	Genes
	hsa-miR-345-5p	GO:0003179	Heart valve morphogenesis	$4.65x10^{-2}$	HEY2/ERG
	hsa-miR-345-5p	GO:0007266	Rho protein signal transduction	$4.65x10^{-2}$	CDC42EP2/NGFR/P2RY8
	hsa-miR-664a-3p	GO:0060712	Spongiotrophoblast layer development	$3.57x10^{-3}$	LIF/NRK/PHLDA2
	hsa-miR-664a-3p	GO:0010976	Positive regulation of neuron projection development	$3.11x10^{-2}$	MAP1B/NTRK2/PAK3/SKIL/NLGN1
	hsa-miR-664a-3p	GO:0033135	Regulation of peptidyl-serine phosphorylation	$3.11x10^{-2}$	LIF/PTGS2/NTRK2/RASSF2
	hsa-miR-664a-3p	GO:0010770	Positive regulation of cell morphogenesis involved in differentiation	$3.11x10^{-2}$	MAP1B/NTRK2/PAK3/SKIL
	hsa-miR-664a-3p	GO:0010769	Regulation of cell morphogenesis involved in differentiation	$3.11x10^{-2}$	MAP1B/NTRK2/PAK3/SKIL/NLGN1
	hsa-let-7e-5p	GO:0010866	Regulation of triglyceride biosynthetic process	$5.26x10^{-3}$	THRSP/DGAT2
	hsa-let-7e-5p	GO:0046890	Regulation of lipid biosynthetic process	$5.26x10^{-3}$	THRSP/SCD/DGAT2
	hsa-let-7e-5p	GO:0019432	Triglyceride biosynthetic process	$5.26x10^{-3}$	THRSP/DGAT2
	hsa-let-7e-5p	GO:0090207	Regulation of triglyceride metabolic process	$5.26x10^{-3}$	THRSP/DGAT2
	hsa-let-7e-5p	GO:0046460	Neutral lipid biosynthetic process	$5.26x10^{-3}$	THRSP/DGAT2
	hsa-miR-212-3p	GO:0050708	Regulation of protein	$5.15x10^{-3}$	SLC2A1/IL1RL1/GPAM/PDE8B
	hsa-miR-212-3p	GO:0002791	Regulation of peptide secretion	$5.15x10^{-3}$	SLC2A1/IL1RL1/GPAM/PDE8B
Down	hsa-miR-130b-5p	GO:0001101	Response to acid chemical	$2.93x10^{-2}$	WNT5A/ACSL1/LEP/PTGFR
	hsa-miR-130b-5p	GO:0043032	Positive regulation of macrophage activation	$2.93x10^{-2}$	WNT5A/IL1RL1
	hsa-miR-130b-5p	GO:0050727	Regulation of inflammatory response	$3.66x10^{-2}$	WNT5A/LEP/CX3CL1/IL1RL1
	hsa-miR-130b-5p	GO:0072606	Interleukin-8 secretion	$3.66x10^{-2}$	WNT5A/LEP
	hsa-miR-130b-5p	GO:0001819	Positive regulation of cytokine production	$3.66x10^{-2}$	WNT5A/LEP/CX3CL1/IL1RL1
	hsa-miR-23a-5p	GO:0006865	Amino acid transport	$2.87x10^{-2}$	LEP/SLC6A6/ATP1A2
	hsa-miR-23a-5p	GO:0051955	Regulation of amino acid transport	$2.87x10^{-2}$	LEP/ATP1A2
	hsa-miR-23a-5p	GO:0006109	Regulation of carbohydrate metabolic process	$2.87x10^{-2}$	LEP/IGFBP5/PFKFB4
	hsa-miR-23a-5p	GO:0019229	Regulation of vasoconstriction	$2.87x10^{-2}$	LEP/ATP1A2
	hsa-miR-23a-5p	GO:0046942	Carboxylic acid transport	$2.87x10^{-2}$	LEP/SLC6A6/ATP1A2
	hsa-miR-23a-5p	GO:0001909	Leukocyte mediated cytotoxicity	$3.30x10^{-2}$	LEP/TREM1
	hsa-miR-23a-5p	GO:0014897	Striated muscle hypertrophy	$3.80x10^{-2}$	LEP/IGFBP5
	hsa-miR-23a-5p	GO:0010906	Regulation of glucose metabolic process	$3.80x10^{-2}$	LEP/IGFBP5
	hsa-miR-23a-5p	GO:0010675	Regulation of cellular carbohydrate metabolic process	$4.72x10^{-2}$	LEP/IGFBP5
	hsa-miR-23b-3p	GO:0007422	Peripheral nervous system development	$4.39x10^{-2}$	ALDH3A2/EDNRB/HOXD10

Table VII. Continued.

Expression	Cluster	ID	Description	Adjusted P-value	Genes
	hsa-miR-302d-3p	GO:0010888	Negative regulation of lipid storage	$3.41x10^{-2}$	LEP/ABCG1
	hsa-miR-302d-3p	GO:0032355	Response to estradiol	$3.41x10^{-2}$	LEP/TXNIP/PTGFR
	hsa-miR-302d-3p	GO:0008203	Cholesterol metabolic process	$3.41x10^{-2}$	VLDLR/LEP/ABCG1
	hsa-miR-302d-3p	GO:1902652	Secondary alcohol metabolic process	$3.41x10^{-2}$	VLDLR/LEP/ABCG1
	hsa-miR-302d-3p	GO:0006869	Lipid transport	$3.41x10^{-2}$	VLDLR/LEP/THRSP/ ABCG1
	hsa-miR-302d-3p	GO:1900015	Regulation of cytokine production involved in inflammatory response	$3.41x10^{-2}$	C5orf30/LEP
	hsa-miR-302d-3p	GO:0046890	Regulation of lipid biosynthetic process	$3.41x10^{-2}$	LEP/THRSP/ABCG1
	hsa-miR-302d-3p	GO:0002534	Cytokine production involved in inflammatory response	$3.41x10^{-2}$	C5orf30/LEP
	hsa-miR-485-3p	GO:0035384	Thioester biosynthetic process	$2.86x10^{-2}$	PDHX/SCD
	hsa-miR-485-3p	GO:0071616	Acyl-CoA biosynthetic process	$2.86x10^{-2}$	PDHX/SCD

GO, Gene Ontology; miR, microRNA.

adipocytes (44). The expression of miR-378a is upregulated in the adipose tissues of high fat diet-induced obese mice, and during the differentiation of preadipocytes (45,46). Investigations of the mechanism have revealed that miR-378 may induce adipogenesis by targeting mitogen-activated protein kinase 1 (45), E2F transcription factor 2 and Ras-related nuclear-binding protein 10 (46). Accordingly, it was hypothesized that hsa-miR-378a-5p may be upregulated in adipocyte differentiated HASCs, which was demonstrated in the present study. However, further experiments are required to confirm the role of this miRNA in HASC differentiation and its targeted interactions with RAC2. There are no previous reports on the roles of GDNF-AS1 in HASC differentiation, indicating it may also be a novel target identified by the present study.

Hub genes CXCL10 in module 2 and EHHADH in module 6 were shown to be respectively regulated by hsa-miR-411-3p and hsa-miR-487a, being involved in inflammatory and amino acid metabolism pathways for HASC differentiation. As reported for LEP above, inflammation promotes the adipocyte differentiation of HASCs, whereas CXCL10 is a well-known pro-inflammatory chemokine (47). Therefore, CXCL10 may be upregulated in adipocyte differentiated HASCs, which was confirmed in the present study. EHHADH has been reported as a downstream target upregulated by PPAR (48). PPAR is an important marker in stimulating adipogenesis (12). EHHADH may also be expressed at a high level in adipocyte differentiated HASCs, which was in consistent with the present study. These two miRNAs regulating CXCL10 and EHHADH have not been demonstrated to be responsible for HASC differentiation, which highlights potential directions in future investigations.

CCNB1, JUN and PTPRC were suggested to be important for adipocyte differentiation from HASCs according to the PPI network analysis. With reference to previous studies, high expression levels of CCNB1 (49) and JUN (50) may be positively associated with the proliferation of stem cells. Generally, the differentiation process can be executed only following weakening of the proliferation ability of stem cells. In the adipocyte differentiation of HASCs, CCNB1 and JUN may be downregulated, which was verified in the present study. PTPRC is also known as CD45, a JAK phosphatase, which negatively regulates cytokine receptor signaling via inhibiting the activity of STAT3 (51,52). According to the findings of LEP above, PTPRC may be downregulated for the adipocyte differentiation of HASCs, which was in line with the results of the present study.

There were some limitations in the present study. First, adipocyte differentiated cells were induced following different culture durations in the GSE57593, GSE25715 and GSE61302 datasets, which may lead to differences in the expression levels of the identified mRNAs, miRNAs and lncRNAs if the same samples were used for their detection. Second, the sample size of each dataset (GSE57593: Four undifferentiated HASCs and six adipocyte differentiated cells; GSE25715: Four undifferentiated HASCs and eight adipocyte differentiated cells: GSE61302: Five undifferentiated HASCs and 10 adipocyte differentiated cells) was small. Additional high-throughput sequencing experiments with larger samples are required to confirm the conclusions. Third, the present study comprised preliminary screening; however, further wet experiments, including quantitative-polymerase chain reaction analysis, western blotting, dual luciferase reporter assays, and knockout or overexpression *in vitro* and *in vivo*, are indispensable to confirm the expression

levels of the identified target genes and validate the regulatory associations between DEMs and DELs/DEGs.

In conclusion, the present study preliminarily identified several crucial DEGs (LEP, RAC2, CXCL10, EHHADH CCNB1, JUN and PTPRC), DEMs (has-miR-130b-5p and has-miR-23a-5p, has-miR-302d-3p, has-miR-378a-5p, hsa-miR-411-3p and hsa-miR-487a) and DELs (RP11-552F3.9, RP11-15A1.7 and GDNF-AS1) for inducing the adipogenic differentiation of HASCs. Among these, the RP11-552F3.9 (or RP11-15A1.7)-hsa-miR-302d-3p-LEP ceRNA interaction axes may be particularly important and represents a novel mechanism for the adipogenic differentiation of HASCs. Further *in vitro* and *in vivo* investigations are required to confirm their roles in breast reconstruction and augmentation.

Acknowledgements

Not applicable.

Funding

No funding was received.

Availability of data and materials

The microarray data GSE57593, GSE25715 and GSE61302 were downloaded from the GEO database in NCBI (www.ncbi.nlm.nih.gov/geo/).

Authors' contributions

ZG and YC conceived and designed the original study. ZG conducted the bioinformatic analysis and drafted the manuscript. YC contributed to the acquisition and interpretation of data and revised the manuscript. Both authors read and approved the final manuscript.

Ethics approval and consent to participate

Not applicable.

Patient consent for publication

Not applicable.

Competing interests

The authors declare that they have no competing interests.

References

1. Ghoncheh M, Pournamdar Z, Salehiniya H: Incidence and mortality and epidemiology of breast cancer in the world. Asian Pac J Cancer Prev 17: 43-46, 2016.
2. Szychta P, Zadrozny M, Rykala J, Banasiak L and Witmanowski H: Autologous fat transfer to the subcutaneous tissue in the context of breast reconstructive procedures. Postepy Dermatol Alergol 33: 323-328, 2016.
3. Soares MA, Ezeamuzie OC, Ham MJ, Duckworth AM, Rabbani PS, Saadeh PB and Ceradini DJ: Targeted protection of donor graft vasculature using a phosphodiesterase inhibitor increases survival and predictability of autologous fat grafts. Plast Reconstr Surg 135: 488-499, 2015.
4. Kølle SF, Fischer-Nielsen A, Mathiasen AB, Elberg JJ, Oliveri RS, Glovinski PV, Kastrup J, Kirchhoff M, Rasmussen BS, Talman ML, *et al*: Enrichment of autologous fat grafts with ex-vivo expanded adipose tissue-derived stem cells for graft survival: A randomised placebo-controlled trial. Lancet 382: 1113-1120, 2013.
5. Sterodimas A, Faria JD, Nicaretta B and Boriani F: Autologous fat transplantation versus adipose-derived stem cell-enriched lipografts: A study. Aesthet Surg J 31: 682-693, 2011.
6. Tan SS, Zhi YN, Zhan W and Rozen W: Role of adipose-derived stem cells in fat grafting and reconstructive surgery. J Cutan Aesthet Surg 9: 152-156, 2016.
7. Feng H, Qiu L, Zhang T, Yu H, Ma X, Su Y, Zheng H, Wang Y and Yi C: Heat-Shock Protein 70 Overexpression in adipose-derived stem cells enhances fat graft survival. Ann Plast Surg 78: 460-466, 2017.
8. Sun X, Zou T, Zuo C, Zhang M, Shi B, Jiang Z, Cui H, Liao X, Li X, Tang Y, *et al*: IL-1α inhibits proliferation and adipogenic differentiation of human adipose-derived mesenchymal stem cells through NF-κB- and ERK1/2- mediated proinflammatory cytokines. Cell Biol Int 42: 794-803 2018.
9. Strong AL, Gimble JM and Bunnell BA: Analysis of the pro- and anti-inflammatory cytokines secreted by adult stem cells during differentiation. Stem Cells Int 2015: 412467, 2015.
10. Satish L, Krill-Burger JM, Gallo PH, Etages SD, Liu F, Philips BJ, Ravuri S, Marra KG, Laframboise WA, Kathju S and Rubin JP: Expression analysis of human adipose-derived stem cells during in vitro differentiation to an adipocyte lineage. BMC Med Genomics 8: 41, 2015.
11. Kang T, Lu W, Xu W, Anderson L, Bacanamwo M, Thompson W, Chen YE and Liu D: MicroRNA-27 (miR-27) targets prohibitin and impairs adipocyte differentiation and mitochondrial function in human adipose-derived stem Cells. J Biol Chem 288: 34394-34402, 2013.
12. Li H, Li T, Wang S, Wei J, Fan J, Li J, Han Q, Liao L, Shao C and Zhao RC: miR-17-5p and miR-106a are involved in the balance between osteogenic and adipogenic differentiation of adipose-derived mesenchymal stem cells. Stem Cell Res 10: 313-324, 2013.
13. Nuermaimaiti N, Liu J, Liang X, Jiao Y, Zhang D, Liu L, Meng X and Guan Y: Effect of lncRNA HOXA11-AS1 on adipocyte differentiation in human adipose-derived stem cells. Biochem Biophys Res Commun 495: 1878-1884, 2018.
14. Huang Y, Jin C, Zheng Y, Li X, Shan Z, Zhang Y, Jia L and Li W: Knockdown of lncRNA MIR31HG inhibits adipocyte differentiation of human adipose-derived stem cells via histone modification of FABP4. Sci Rep 7: 8080, 2017.
15. Shang G, Wang Y, Xu Y, Zhang S, Sun X, Guan H, Zhao X, Wang Y, Li Y and Zhao G: Long non-coding RNA TCONS_00041960 enhances osteogenesis and inhibits adipogenesis of rat bone marrow mesenchymal stem cell by targeting miR-204-5p and miR-125a-3p. J Cell Physiol 233: 6041-6051, 2018.
16. Li M, Xie Z, Wang P, Li J, Liu W, Tang S, Liu Z, Wu X, Wu Y and Shen H: The long noncoding RNA GAS5 negatively regulates the adipogenic differentiation of MSCs by modulating the miR-18a/CTGF axis as a ceRNA. Cell Death Dis 9: 554, 2007.
17. Irizarry RA, Hobbs B, Collin F, Beazer-Barclay YD, Antonellis KJ, Scherf U and Speed TP: Exploration, normalization, and summaries of high density oligonucleotide array probe level data. Biostatistics 4: 249-264, 2003.
18. Ritchie ME, Phipson B, Wu D, Hu Y, Law CW, Shi W and Smyth GK: limma powers differential expression analyses for RNA-sequencing and microarray studies. Nucleic Acids Res 43: e47, 2015.
19. Thissen D, Steinberg L and Kuang D: Quick and easy implementation of the benjamini-hochberg procedure for controlling the false positive rate in multiple comparisons. J Educ Behav Stat 27: 77-83, 2002.
20. Szklarczyk D, Franceschini A, Wyder S, Forslund K, Heller D, Huerta-Cepas J, Simonovic M, Roth A, Santos A, Tsafou KP, *et al*: STRING v10: Protein-protein interaction networks, integrated over the tree of life. Nucleic Acids Res 43 (Database Issue): D447-D452, 2015.
21. Kohl M, Wiese S and Warscheid B: Cytoscape: Software for visualization and analysis of biological networks. Methods Mol Biol 696: 291-303, 2011.
22. Tang Y, Li M, Wang J, Pan Y and Wu FX: CytoNCA: A cytoscape plugin for centrality analysis and evaluation of protein interaction networks. Biosystems 127: 67-72, 2015.

23. Bader GD and Hogue CW: An automated method for finding molecular complexes in large protein interaction networks. BMC Bioinformatics 4: 2, 2003.
24. Dweep H and Gretz N: miRWalk2. 0: A comprehensive atlas of microRNA-target interactions. Nat Methods 12: 697, 2015.
25. Das S, Ghosal S, Sen R and Chakrabarti J: lnCeDB: Database of human long noncoding RNA acting as competing endogenous RNA. PLoS One 9: e98965, 2014.
26. Kleiman A, Keats EC, Chan NG and Khan ZA: Elevated IGF2 prevents leptin induction and terminal adipocyte differentiation in hemangioma stem cells. Exp Mol Pathol 94: 126-136, 2013.
27. Lee HS, Jang H, Jin OP, Choi J, Youm JH and Hong ST: Effect of leptin on the differentiation of adipose tissue-derived and bone marrow stromal cells into adipocytes. Tissue Eng Regen Med 6: 1134-1138, 2009.
28. Thomas T, Gori F, Khosla S, Jensen MD, Burguera B and Riggs BL: Leptin acts on human marrow stromal cells to enhance differentiation to osteoblasts and to inhibit differentiation to adipocytes. Endocrinology 140: 1630-1638, 1999.
29. Um S, Choi JR, Lee JH, Zhang Q and Seo B: Effect of leptin on differentiation of human dental stem cells. Oral Dis 17: 662-669, 2011.
30. Wang YN, Yang M, Yu LH, Guo J, Chen N and He L: Leptin play the key role in astroglial differentiation of mouse neural stem cells and regulated the STAT3 signaling through Jak-STAT3 pathway. Sichuan Da Xue Xue Bao Yi Xue Ban 45: 552-556, 2014 (In Chinese).
31. Georas SN, Cumberland JE, Burke TF, Chen R, Schindler U and Casolaro V: Stat6 inhibits human interleukin-4 promoter activity in T cells. Blood 92: 4529-4538, 1998.
32. Tsao CH, Shiau MY, Chuang PH, Chang YH and Hwang J: Interleukin-4 regulates lipid metabolism by inhibiting adipogenesis and promoting lipolysis. J Lipid Res 55: 385-397, 2014.
33. Shin KK, Kim YS, Kim JY, Bae YC and Jung JS: miR-137 controls proliferation and differentiation of human adipose tissue stromal cells. Cell Physiol Biochem 33: 758-768, 2014.
34. Huang S, Wang S, Bian C, Yang Z, Zhou H, Zeng Y, Li H, Han Q and Zhao RC: Upregulation of miR-22 promotes osteogenic differentiation and inhibits adipogenic differentiation of human adipose tissue-derived mesenchymal stem cells by repressing HDAC6 protein expression. Stem Cells Dev 21: 2531-2540, 2012.
35. Yang Z, Bian C, Zhou H, Huang S, Wang S, Liao L and Zhao RC: MicroRNA hsa-miR-138 inhibits adipogenic differentiation of human adipose tissue-derived mesenchymal stem cells through adenovirus EID-1. Stem Cells Dev 20: 259-267, 2011.
36. Kim YJ, Hwang SJ, Yong CB and Jin SJ: MiR-21 regulates adipogenic differentiation through the modulation of TGF-β signaling in mesenchymal stem cells derived from human adipose tissue. Stem Cells 27: 3093-3102, 2009.
37. Lee EK, Mi JL, Abdelmohsen K, Kim W, Kim MM, Srikantan S, Martindale JL, Hutchison ER, Kim HH, Marasa BS, *et al*: miR-130 suppresses adipogenesis by inhibiting peroxisome proliferator-activated receptor gamma expression. Mol Cell Biol 31: 626-638, 2011.
38. Guo Q, Chen Y, Guo L, Jiang T and Lin Z: miR-23a/b regulates the balance between osteoblast and adipocyte differentiation in bone marrow mesenchymal stem cells. Bone Res 4: 16022, 2016.
39. Kang JM, Han M, Park IS, Jung Y, Kim SH and Kim SH: Adhesion and differentiation of adipose-derived stem cells on a substrate with immobilized fibroblast growth factor. Acta Biomater 8: 1759-1767, 2012.
40. Young DA, Yu SC, Engler AJ and Christman KL: Stimulation of adipogenesis of adult adipose-derived stem cells using substrates that mimic the stiffness of adipose tissue. Biomaterials 34: 8581-8588, 2013.
41. Bae YH, Mui KL, Hsu BY, Liu SL, Cretu A, Razinia Z, Xu T, Puré E and Assoian RK: A FAK-Cas-Rac-lamellipodin signaling module transduces extracellular matrix stiffness into mechanosensitive cell cycling. Sci Signal 7: ra57, 2014.
42. Hyväri L, Ojansivu M, Juntunen M, Kartasalo K, Miettinen S and Vanhatupa S: Focal adhesion kinase and ROCK signaling are switch-like regulators of human adipose stem cell differentiation towards osteogenic and adipogenic lineages. Stem Cells Int 2018: 2190657, 2018.
43. Le TN, Oscar C, Mouw JK, Sharmila C, Hector M, Angel M, Jillian R, Keely PJ, Weaver VM and Lindsay H: Loss of miR-203 regulates cell shape and matrix adhesion through ROBO1/Rac/FAK in response to stiffness. J Cell Biol 212: 707-719, 2016.
44. Xu LL, Shi CM, Xu GF, Chen L, Zhu LL, Zhu L, Guo XR, Xu MY and Ji CB: TNF-α, IL-6, and leptin increase the expression of miR-378, an adipogenesis-related microRNA in human adipocytes. Cell Biochem Biophys 70: 771-776, 2014.
45. Huang N, Wang J, Xie W, Lyu Q, Wu J, He J, Qiu W, Xu N and Zhang Y: MiR-378a-3p enhances adipogenesis by targeting mitogen-activated protein kinase 1. Biochem Biophys Res Commun 457: 37-42, 2015.
46. Liu SY, Zhang YY, Gao Y, Zhang LJ, Chen HY, Zhou Q, Chai ML, Li QY, Jiang H, Yuan B, *et al*: MiR-378 plays an important role in the differentiation of bovine preadipocytes. Cell Physiol Biochem 36: 1552-1562, 2015.
47. Gao B, Lin J, Jiang Z, Yang Z, Yu H, Ding L, Yu M, Cui Q, Dunavin N, Zhang M and Li M: Upregulation of chemokine CXCL10 enhances chronic pulmonary inflammation in tree shrew collagen-induced arthritis. Sci Rep 8: 9993, 2018.
48. Lu YF, Xu YY, Jin F, Wu Q, Shi JS and Liu J: Icariin is a PPARα activator inducing lipid metabolic gene expression in mice. Molecules 19: 18179, 2014.
49. Fujii-Yamamoto H, Kim JM, Arai K and Masai H: Cell cycle and developmental regulations of replication factors in mouse embryonic stem cells. J Biol Chem 280: 12976-12987, 2005.
50. Jiao X, Katiyar S, Willmarth NE, Liu M, Ma X, Flomenberg N, Lisanti MP and Pestell RG: c-Jun induces mammary epithelial cellular invasion and breast cancer stem cell expansion. J Biol Chem 285: 8218-8226, 2010.
51. Irie-Sasaki J, Sasaki T, Matsumoto W, Opavsky A, Cheng M, Welstead G, Griffiths E, Krawczyk C, Richardson CD, Aitken K, *et al*: CD45 is a JAK phosphatase and negatively regulates cytokine receptor signalling. Nature 409: 349-354, 2001.
52. Kumar V, Cheng P, Condamine T, Mony S, Languino L, McCaffrey J, Hockstein N, Guarino M, Masters G, Penman E, *et al*: CD45 phosphatase inhibits STAT3 transcription factor activity in myeloid cells and promotes tumor-associated macrophage differentiation. Immunity 44: 303-315, 2016.